

Impact of Inhomogeneous Strain on the Valence Band Structures of Ge-Si Core-Shell Nanowires

Yuhui He¹, Chun Fan², Yu Ning Zhao¹, Gang Du¹, Xiao Yan Liu^{1,*} and Ruqi Han¹

¹Institute of Microelectronics, Peking University, Beijing 100871, China

²Computer Center of Peking University, Beijing 100871, China

* Correspondence: xyliu@ime.pku.edu.cn

Abstract—We report on a theoretical study of the valence band structures of germanium-silicon core-shell nanowires based on a $6 \times 6 \mathbf{k}\cdot\mathbf{p}$ model. We take into account the inhomogeneous strain effects induced by the lattice mismatches between germanium and silicon. We find that the top subband ends drift back to Γ point, and the effective masses of more subbands begin to decrease when the shell thickness increases.

Keywords-strain effect; core-shell nanowire; valence band

I. INTRODUCTION

Nowadays carbon nanotubes and nanowires (NWs) have been the focus of studies as potential building blocks for nanodevices [1]. More complex core-shell (C-S) and core-multishell semiconductor NWs have been prepared experimentally by growing epitaxial shell(s) along the radial orientation of the NWs [2-5]. Very high carrier mobility have been demonstrated, which is attributed to the confinement of holes in the quantum well of core NW, the reduction of surface roughness scattering and strain effect induced by core-shell lattice mismatches. As in Ge-Si C-S nanowires, the 0.5 eV band offset between Ge core and Si shell induces a quantum well in Ge core and makes low-energy hole transport concentrate there. Besides, the lattice mismatches between Ge core and Si shell induce pseudomorphic strain in Ge core and provide more flexibility in valence band structure modulations.

To quantitatively investigate hole transport properties in the Ge-Si C-S NWs, valence band structure calculation is essential. At current stage *Ab initio* study [6,7] is difficult to deal with NWs with diameters larger than 3-4 nm. Tight-binding approach [8,9] faces similar difficulty. Here we present our calculation based on a $6 \times 6 \mathbf{k}\cdot\mathbf{p}$ model taking account of inhomogeneous strain effect. First we simulate the strain distribution in the NW by using an elasticity continuum model and then calculate the NW valence band structure by employing a strained Hamiltonian in the $\mathbf{k}\cdot\mathbf{p}$ framework. Finally we analyze the dependence of this strain-induced modulation ON the NW shell thicknesses.

II. STRAIN SIMULATION

We employ a continuum elasticity model [10] for the strain calculation where the strain energy density $u_0(\mathbf{r}) = \boldsymbol{\epsilon}^T \mathbf{C} \boldsymbol{\epsilon}/2$. $\boldsymbol{\epsilon} = [\epsilon_{xx} \ \epsilon_{yy} \ \epsilon_{zz} \ \epsilon_{yz} \ \epsilon_{xz} \ \epsilon_{xy}]$, and \mathbf{C} is the elastic modulus tensor. Since Ge-Si core-shell nanowires are grown along $z = [1 \ 1 \ 0]$ orientation, we make a coordinate transform from an ordinary

coordinate where $x = [1 \ 0 \ 0]$, $y = [0 \ 1 \ 0]$ and $z = [0 \ 0 \ 1]$ to a new coordinate where $x = [1 \ 1 -\sqrt{2}]$, $y = [-1 \ 1 -\sqrt{2}]$ and $z = [1 \ 1 \ 0]$. Then we write the total elastic strain energy U as two parts [11, 12] $U = U_s + U_c$, where U_s is the elastic strain energy in the shell:

$$U_s = \int ds \{ D_1^s (\Delta \epsilon_{xx}^2 + \Delta \epsilon_{yy}^2) + D_2^s (a_z/a_z^s - 1)^2 + D_3^s \epsilon_{xy}^2 + D_4^s \Delta \epsilon_{xx} \Delta \epsilon_{yy} + (\Delta \epsilon_{xx} + \Delta \epsilon_{yy}) [D_5^s (a_z/a_z^s - 1) + D_6^s \epsilon_{xy}] \} / 2, \quad (1)$$

where

$$D_1 = (6C_{11} + 10C_{12} + 5C_{44})/16,$$

$$D_2 = (2C_{11} + 2C_{12} + C_{44})/4,$$

$$D_3 = (6C_{11} - 6C_{12} + C_{44})/4,$$

$$D_4 = (6C_{11} + 10C_{12} - 3C_{44})/8,$$

$$D_5 = (2C_{11} + 6C_{12} - C_{44})/4,$$

$$D_6 = (2C_{11} - 2C_{12} - C_{44})/4,$$

$$\Delta \epsilon_{ii} = \epsilon_{ii} - \epsilon_{ii}^s \text{ and } \epsilon_{ii}^s = (a_i^s - a_i^c)/a_i^c,$$

and U_c is the elastic strain energy in the core which has a similar form as U_s except $\epsilon_{ii}^c = 0$.

In the above derivation, we have assumed that the NW is long enough. Thus the strain tensor ϵ_{ij} is independent on z because of the translational invariance over NW axial orientation. Besides, the Ge core and Si shell share the same lattice distance a_z everywhere in the NW. Otherwise it would break the translational invariance along NW axis and such a lattice could not be stable. For similar considerations, we have taken the shear strain tensor ϵ_{xz} and ϵ_{yz} to be zero.

Then we calculate the strain energy minimal via finite-element method, and obtain the corresponding strain tensor distribution $\epsilon_{ij}(\mathbf{r})$. Here all the material parameters used are taken from ref. 13.

Figure 1a, 1b and 1c plot the strain energy $U(\mathbf{r})$ in the NW cross-section (x - y plain) with the same 6-nm Ge core radius and with various Si shell thicknesses. Figure 1d, 1e and 1f plot strain tensor distribution $\epsilon_{xx}(\mathbf{r})$, $\epsilon_{yy}(\mathbf{r})$ and $\epsilon_{xy}(\mathbf{r})$ for a NW with 6-nm core radius and 2-nm shell thickness.

Compared to that in the shell, both $U(\mathbf{r})$ and $\epsilon_{ij}(\mathbf{r})$ are very small and homogeneous in the core, which can be understood from the eggshell principle in engineering: no matter how much stress you put on it, the egg disperses the stress over the whole shell homogeneously and keeps unbroken as long as the

shell is round and perfect. Furthermore, $U(\mathbf{r})$ in the shell has a cubic symmetry because of the equivalence between lattice orientations $x=[1 \ 1 -\sqrt{2}]$ and $y=[-1 \ 1 -\sqrt{2}]$.

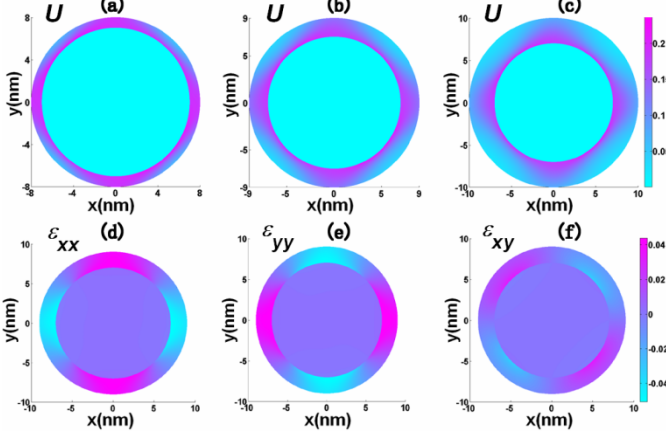


Figure 1. Strain energy distribution $U(\mathbf{r})$ in the 6-nm core radius nanowire cross sections, with various outer radii from 7 nm (a) to 8 nm (b) to 9 nm (c). Strain tensor $\epsilon_{xx}(\mathbf{r})$ (d), $\epsilon_{yy}(\mathbf{r})$ (e) and $\epsilon_{xy}(\mathbf{r})$ (f) distributions in a 6-nm core radius and 2-nm shell thickness NW.

Besides, we can see along x -oriented interface between Ge core and Si shell, $\epsilon_{xx}(\mathbf{r})$ is negative in the core side while positive in the shell side. This means at these places the Ge core feels a compressive strain, while the Si shell feels a tensile strain. It is just as expected since Ge has a larger lattice constant than Si does. Similar things happen to $\epsilon_{yy}(\mathbf{r})$ and $\epsilon_{xy}(\mathbf{r})$. Last but not least, the strain gradually relaxes along the radial orientation in the shell as the shell gets thicker.

III. STRAINED VALENCE BAND CALCULATION

We employ a 6×6 $\mathbf{k} \cdot \mathbf{p}$ Hamiltonian for light hole (LH), heavy hole (HH) and split-off (SO) hole band calculation. Here we take into account SO bands because it is believed that strain induced extra couplings between LH , HH and SO will have untrivial effects on the top LH and HH band structures [14]. We assume that the nanowires can be well approximated with concentric cylinders, and employ the basis functions as follows:

$$\Phi_{l,m,k_z}(r, \theta, z) = A_{l,m} J_l(\alpha_m^l r/R) e^{il\theta} \exp(ik_z z) / L_z \quad (2)$$

where α_m^l is the m -th zero of l -order Bessel function $J_l(r)$, $A_{l,m}$ is the normalization parameter, L_z is nanowire length and R is the full radius of the nanowire.

Then we describe the first-order strain effect in such radial heterostructures with a perturbation Hamiltonian H'_{st} [15]:

$$\begin{bmatrix} P-Q & -S & R & 0 & -\frac{S}{\sqrt{2}} & \sqrt{2}R \\ -S^+ & P+Q & 0 & R & \sqrt{2}Q & \sqrt{\frac{3}{2}}S \\ R^+ & 0 & P+Q & S & \sqrt{\frac{3}{2}}S^+ & -\sqrt{2}Q \\ 0 & R^+ & S^+ & P-Q & -\sqrt{2}R^+ & -\frac{S^+}{\sqrt{2}} \\ -\frac{S^+}{\sqrt{2}} & \sqrt{2}Q & \sqrt{\frac{3}{2}}S & -\sqrt{2}R & P+\Delta & 0 \\ \sqrt{2}R^+ & \sqrt{\frac{3}{2}}S^+ & -\sqrt{2}Q & -\frac{S}{\sqrt{2}} & 0 & P+\Delta \end{bmatrix}, \quad (3)$$

where $P = -a'(\epsilon_{xx} + \epsilon_{yy} + \epsilon_{zz})$,

$$q = b'(-\epsilon_{xx}/4 - \epsilon_{yy}/4 + \epsilon_{zz}/2 - 3\epsilon_{xy}/2),$$

$$s = d'(I+i)(\epsilon_{xx} - \epsilon_{yy})/(2\sqrt{2}),$$

$$r = id'(\epsilon_{xx}/4 + \epsilon_{yy}/4 - \epsilon_{zz}/2 - \epsilon_{xy}/2).$$

Here a' , b' and d' are modified valence deformation potentials: $a' = a_v - 2\Delta/9$, $b' = b - 2\Delta/9$ and $d' = d_v - 2\Delta/9$.

We further adapt a phenomenological treatment with the inhomogeneous strain effect by changing strain tensor ϵ_{ij} to $\epsilon_{ij}(\mathbf{r})$ [16].

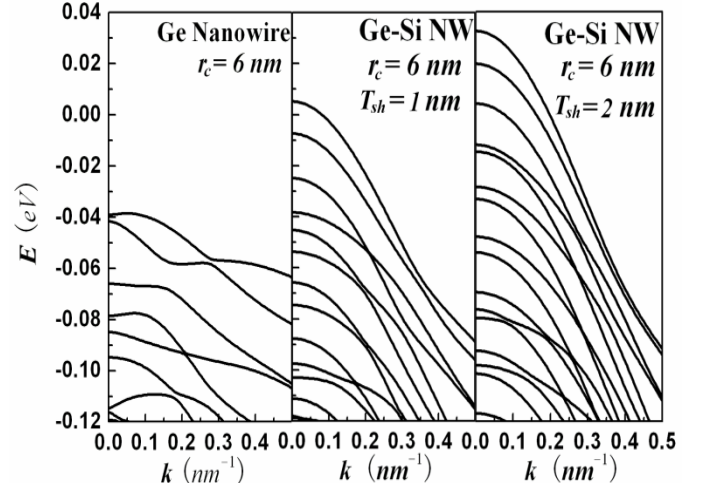


Figure 2. Top valence subband structures of Ge-Si NWs with 6-nm core radius, and with 0-nm (Left), 1-nm (Middle) and 2-nm (Right) shell thickness.

Fig. 2a plots the top valence subbands of a 6-nm radius pure Ge NW. As a comparison Fig. 2b and Fig. 2c plot that with the same Ge core radius and with 1-nm and 2-nm Si shell thickness. With strain effect taken into account in the latter case, we observe some substantial changes: those subband ends drifting away from Γ -point in the pure Ge NW have now returned. Besides, the effective masses of the above subbands in the pure Ge NW should have significant ratio as HH while in the strained NW they all turn to be that of LH. All of these

would have profound effects on the hole transport properties and optical properties.

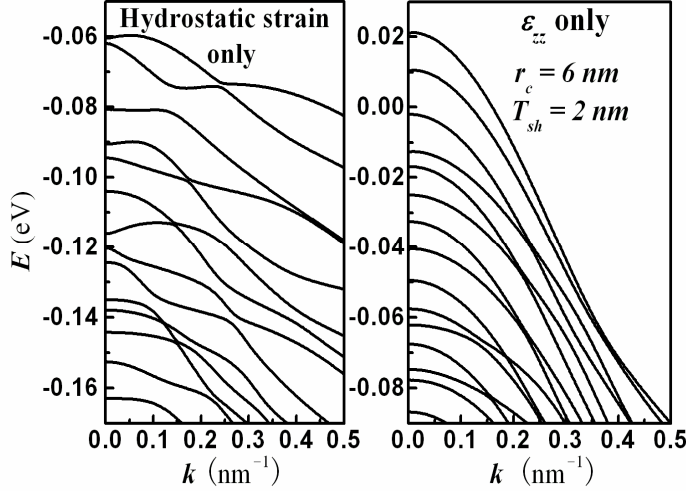


Figure 3. Top valence subbands of Ge-Si C-S NWs with $r_c = 6 \text{ nm}$ and $T_{sh} = 2 \text{ nm}$ by considering hydrostatic strain only (left), and by considering axial strain ε_{zz} only (right).

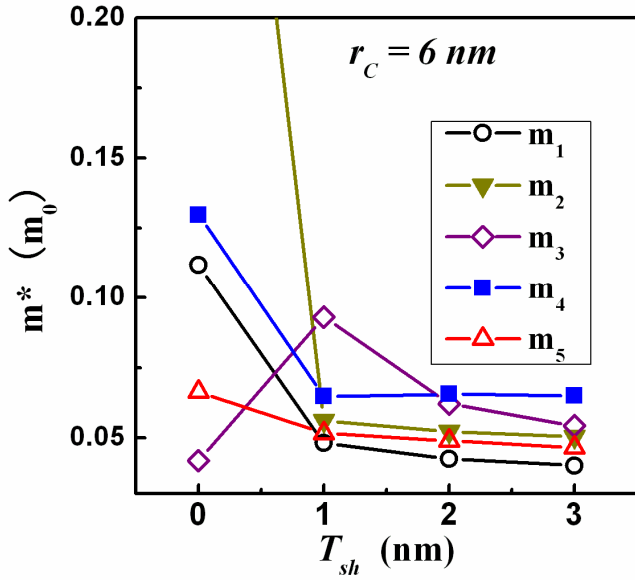


Figure 4. Effective masses m^* of top five subbands versus shell thickness T_{sh} for Ge-Si C-S NWs with radius $r_c = 6 \text{ nm}$.

To further investigate different strain component contributions, we show the valence band structures considering hydrostatic strain component ($\varepsilon_{xx} + \varepsilon_{yy} + \varepsilon_{zz}$) and considering only axial strain component ε_{zz} in Fig. 3a and 3b. Fig. 3a shows that the hydrostatic strain does not have apparent band warping effect. Instead, it induces a total downwards shifting of the subbands. This is in accordance with previous theoretical analysis [17]. Here it is worth mentioning that the top subbands undergo upward shifting when the full strain has been taken into account. Thus we find that it is the off-diagonal shear strain component that causes the subband upward shifting. Fig.3b shows that the axial strain component ε_{zz} contributes the most to the band warping. This is just as expected because ε_{zz} is

much larger than the in-plain strain tensor components ε_{xx} , ε_{yy} and ε_{xy} since the NW is assumed to be infinite long in the simulation.

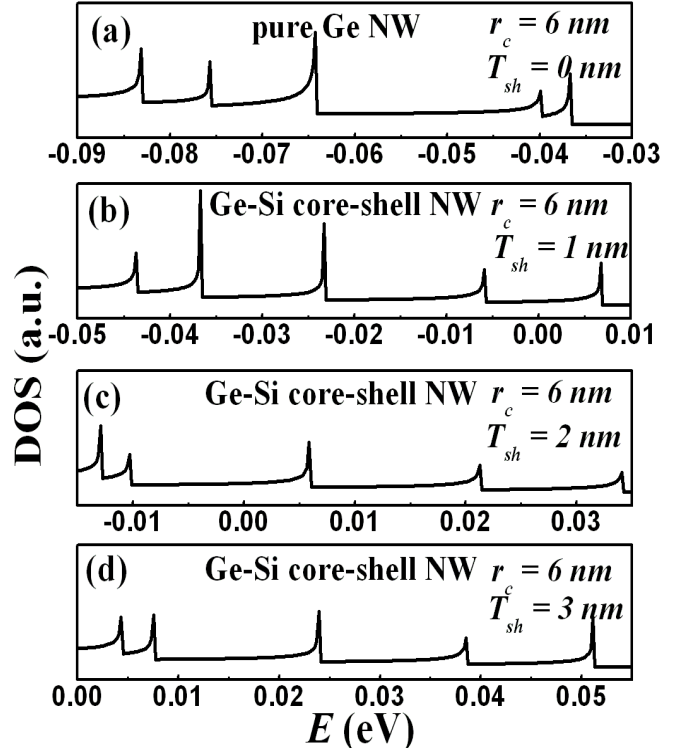


Figure 5. Top parts of densities of states (DOS) of Ge-Si C-S NW with $r_c = 6 \text{ nm}$ and with various T_{sh} from 0 nm (a) to 1 nm (b), 2 nm (c) and 3 nm (d).

Fig. 4 and 5 plot the variance of effective masses and densities of states (DOS) of the top Ge subbands with increasing Si shell thicknesses from. We employ parabola approximation for subband en(kz) in the low energy range and write DOS as

$$n(\varepsilon) \propto \sum_i \theta(\varepsilon_i^0 - \varepsilon) \cdot [m_i^*/(\varepsilon_i^0 - \varepsilon)]^{1/2}. \quad (4)$$

Here ε_i^0 is i -th subband edge, m_i^* is the effective mass at i -th subband edge. Therefore the positions of the peaks in the DOS diagram point out ε_i^0 , while the heights and curvatures depict the magnitude of m_i^* . We find that the top subbands keep upper shifting as the shell goes thicker, because of the larger strain-induced repellent from thicker Si shell. Besides, the heights of the peaks undergo some obvious changes. A very interesting phenomenon we find is that more top subbands will have effective masses as LH as the Si shell thickness increases. Experimentally it means that we would be able to tune the hole transport properties by controlling the growth of Si shell thickness. We also obtain the subband spacing $\Delta E_{1,2} \approx 11 \text{ meV}$, while experimental values [3] are about 25 meV . We attribute these mismatches to the additional charging energy ΔE_C in the experiments: the finite-length Ge-Si C-S NW measured has a capacitance $C \approx 10 \text{ aF}$ so that $\Delta E_C \approx 9 \text{ meV}$. Therefore, our result is more close to experimental estimation than that simulated without strain effect ($\Delta E_{1,2} \approx 2 \text{ meV}$).

IV. CONCLUSION

We have modeled and calculated the valence band structures of Ge-Si core-shell nanowires with a 6×6 $k\cdot p$ model, including the inhomogeneous strain effects. We have found that strain-induced band structure modulations put the subband edges of the core back to Γ -point, and make the top subband have effective masses as light holes. Our calculations meet with experimental observations better taking single-electron charging effect into account, and should be useful for the future device design.

ACKNOWLEDGMENT

This work is supported by NKBRP2006CB302705 and 107003.

REFERENCES

- [1] International Technology Roadmap for Semiconductors, 2006
- [2] L. J. Lauhon, M. S. Gudiksen, D. Wang and C. M. Lieber, "Epitaxial core/shell and core/multishell nanowire heterostructures," *Nature*, vol. 420, pp. 57-61, Nov. 2002.
- [3] W. Lu, J. Xiang, B. P. Timko, Y. Wu and C. M. Lieber, "One-dimensional hole gas in germanium-silicon nanowire heterostructures," *PNAS*, vol. 102, pp. 10046-10051, Jul. 2005
- [4] K. Tateno, H. Gotoh, and Y. Watanabe, *Appl. Phys. Lett.*, "GaAs/AlGaAs nanowires capped with AlGaAs layers on GaAs(311)B substrates," vol 85, no. 10, pp. 1808-1810, Sept.2004.
- [5] N. Sköld, L. S. Karlsson, M. W. Larsson, M.-E. Pistol, W. Seifert, J. Tragardh and L. Samuelson, "Growth and Optical Properties of Strained GaAs-GaxIn_{1-x}P Core-Shell Nanowires," *Nano Lett.*, vol. 5, no. 10, pp. 1943-1947, Nov. 2005.
- [6] J. T. Arantes and A. Fazzio, "Theoretical investigations of Ge nanowires grown along the [110] and [111] directions," *Nanotechnology*, vol 18, pp. 295706, 2007
- [7] M. Nollan, S. O. Callaghan, G. Fagas, J. C. Greer and T. Frauenheim, "Silicon Nanowire Band Gap Modification," *Nano Lett.*, vol 7, pp. 34-38, Jan. 2007
- [8] J. Wang, A. Rahman, A. Ghosh, G. Klimeck and M. Lundstrom, "Performance evaluation of ballistic silicon nanowire transistors with atomic-basis dispersion relations," *Appl. Phys. Lett.* 86, pp. 093113-093115, Feb. 2005
- [9] Y. M. Niquet, "Effects of a Shell on the Electronic Properties of Nanowire Superlattices," *Nano Lett.* 7, pp. 1105-1109, Mar. 2007
- [10] L. Landau and E. Lifshitz, *Theory of Elasticity*, Butterworth-Heinemann, Oxford , 1986
- [11] C. Pryor, J. Kim, L. W. Wang, A. J. Williamson, and A. Zunger, *J. Appl. Phys.*, "Comparison of two methods for describing the strain profiles in quantum dots," vol. 83, pp. 2548-2554, Mar. 1998
- [12] B. Jogai, "Three-dimensional strain field calculations in coupled InAs-GaAs quantum dots," *J. Appl. Phys.*, vol. 88, pp. 5050-5055, Nov. 2000
- [13] M. V. Fischetti and S. E. Laux, "Band structure, deformation potentials, and carrier mobility in strained Si, Ge, and SiGe alloys," *J. Appl. Phys.*, vol. 80, pp. 2234-2252, Aug. 1997
- [14] C. Y. -P. Chao and S. L. Chuang, "Spin-orbit-coupling effects on the valence-band structure of strained semiconductor quantum wells," *Phys. Rev. B*, vol.46, pp. 4110-4122, Aug. 1992
- [15] T. Bahder, "Eight-band $k\cdot p$ model of strained zinc-blende crystals," *Phys. Rev. B*, vol. 41, pp. 11992-12001, Jun. 1992
- [16] Y. Zhang, "Motion of electrons in semiconductors under inhomogeneous strain with application to laterally confined quantum wells," *Phys. Rev. B*, vol. 49, 14352-14366, May 1994
- [17] Y. Sun, S. E. Thompson and T. Nishida, "Physics of strain effects in semiconductors and metal-oxide-semiconductor field-effect transistors", *J. Appl. Phys.*, vol. 101, pp. 104503, May 2007